



# Ill-Conditioning and Bandwidth Expansion in Linear Prediction of Speech

*Peter Kabal*

Department of Electrical & Computer Engineering  
McGill University  
Montreal, Canada

February 2003

---

© 2003 Peter Kabal

### Abstract

This report examines schemes that modify linear prediction (LP) analysis for speech signals. First techniques which improve the conditioning of the LP equations are examined. White noise compensation for the correlations is justified from the point of view of reducing the range of values which the predictor coefficients can take on. A number of other techniques which modify the correlations are investigated (highpass noise, selective power spectrum modification). The efficacy of these procedures is measured over a large speech database. The results show that white noise compensation is the method of choice — it is both effective and simple.

Other methods to prematurely terminate the iterative solution of the correlation equations (Durbin recursion) to circumvent problems of ill-conditioning are also investigated.

The report also considers the bandwidth expansion of digital filters which have resonances. In speech coding such resonances correspond to the formant frequencies. Bandwidth expansion of the LP filter serves to avoid unnatural sharp resonances that may be artefacts of pitch and formant interaction. Lag windowing of the correlation values has been used with the aim of both bandwidth expansion and helping the conditioning of the LP equations. Experiments show that the benefit for conditioning is minimal. This report also discusses bandwidth expansion of the prediction coefficients after LP analysis using radial scaling of the  $z$ -transform. A simple new formula is given which can be used to estimate the bandwidth expansion.

# Ill-Conditioning and Bandwidth Expansion in Linear Prediction of Speech

## 1 Introduction

This report examines techniques which have been employed to modify the linear prediction (LP) analysis of speech signals. One goal of this work is to evaluate methods to improve the conditioning of the LP equations. A motivation for doing so is to limit the dynamic range of the resulting prediction coefficients (for fixed-point implementations). A number of techniques to improve conditioning are described and evaluated.

Secondly, there are a number of approaches to bandwidth expansion of the resonances of LP spectral models. The use of some of these methods has also been proposed to reduce the possibility of ill-conditioning. Indeed this link between bandwidth expansion and improving the conditioning of the LP equations was a starting point for this work. In speech coding resonances correspond to the formant frequencies. Bandwidth expansion is used to dampen the resonances. Modern speech coders employ bandwidth expansion in two places: lag windowing of the correlations before linear predictive (LP) analysis and/or modification of the LP coefficients.

## 2 Linear Predictive Analysis

Linear predictive analysis fits an all-pole model to the local spectrum of a (speech) signal. The model is derived from the autocorrelation sequence of a segment of the speech. The LP spectral fit is determined by solving a set of linear equations based on the correlation values.

Let the input signal be  $x[n]$ . This signal is windowed to give a frame of data to be analyzed,

$$x_w[n] = w[n] x[n]. \quad (1)$$

The linear prediction formulation minimizes the difference between the windowed signal and a

linear combination of past values of the windowed signal,

$$e[n] = x_w[n] - \sum_{k=1}^{N_p} p_k x_w[n-k]. \quad (2)$$

The goal is to minimize the total squared error,

$$\varepsilon = \sum_{n=-\infty}^{\infty} |e[n]|^2. \quad (3)$$

For the case that the window is finite in length, the terms in the sum for the squared error will be non-zero only over a finite interval.

The predictor coefficients ( $p_k$ ) which minimize  $\varepsilon$  can be found from the following set of equations

$$\begin{bmatrix} r[0] & r[1] & \cdots & r[N_p - 1] \\ r[1] & r[0] & \cdots & r[N_p - 2] \\ \vdots & \vdots & \ddots & \vdots \\ r[N_p - 1] & r[N_p - 2] & \cdots & r[0] \end{bmatrix} \begin{bmatrix} p_1 \\ p_2 \\ \vdots \\ p_{N_p} \end{bmatrix} = \begin{bmatrix} r[1] \\ r[2] \\ \vdots \\ r[N_p] \end{bmatrix}. \quad (4)$$

The autocorrelation values are given by

$$r[k] = \sum_{n=-\infty}^{\infty} x_w[n] x_w[n-k]. \quad (5)$$

For finite length windows, the sum needs be evaluated only over a finite interval — the rest of the correlation coefficients will be zero. In vector-matrix notation, the correlation (LP) equations can be written as

$$\mathbf{R}\mathbf{p} = \mathbf{r}. \quad (6)$$

This equation gives the predictor coefficients which minimize the squared error. We will also need to measure the mean-square error for other than the optimal predictor coefficients. The squared error for an arbitrary  $\mathbf{p}$  is

$$\varepsilon = r[0] - 2\mathbf{p}^T \mathbf{r} + \mathbf{p}^T \mathbf{R}\mathbf{p}. \quad (7)$$

Let the prediction error filter be denoted by  $A(z)$ ,

$$A(z) = 1 - \sum_{k=1}^{N_p} p_k z^{-k}. \quad (8)$$

The autocorrelation formulation for the optimal prediction coefficients gives a matrix  $\mathbf{R}$  which is Toeplitz. The Levinson-Durbin algorithm can be used to efficiently solve for the predictor coefficients. The prediction error filter ( $A(z)$ ) will be minimum phase and the corresponding synthesis filter ( $1/A(z)$ ) will be stable.

## 2.1 Conditioning and Predictor Coefficient Values

Of some importance for implementations using fixed-point arithmetic is the dynamic range of the predictor coefficients. If the roots of the prediction error filter are denoted as  $z_n$ , we can write the prediction error filter as a product of its root polynomials,

$$A(z) = \prod_{n=1}^{N_p} (1 - z_n z^{-1}). \quad (9)$$

The  $k$ 'th coefficient of  $A(z)$  in the expression of Eq. (8),  $p_k$ , is the coefficient of  $z^{-k}$ . This power of  $z^{-1}$  appears as the product of  $k$  roots from Eq. (9). For the  $k$ 'th coefficient, there are  $\binom{N_p}{k}$  such products. Since the roots have magnitude less than one (for stability of the synthesis filter), the products all have magnitude less than unity. The largest possible value for a coefficient occurs for coefficient  $N_p/2$  and is  $\binom{N_p}{k}$  when all roots have unit magnitude. For the case of  $N_p = 10$ , common for speech coders, the predictor coefficients have a magnitude which is bounded by 252.

Many modern speech coders (G.729 [1] and SMV [2], for example) store the predictor coefficients in 16-bit fixed-point, with 12 fractional bits (Q12 format). Putting aside one bit for the sign, this leaves 3 bits for the integer part of the representation. The Q12 format can only represent predictor values with values in the range  $[-8, 8)$ . We will measure the effectiveness of methods for conditioning the LP equations in terms of the loss in performance required to bring the predictor coefficients into this range.

Problems with large predictor coefficient values will be worst for systems with singularities near the unit circle. These are the systems that are most predictable. On the other hand, a system with uncorrelated data will have all predictor coefficients equal to zero. The numerical condition of a system of equations can be measured by the condition number. The 2-norm form of the condition number is the ratio of largest eigenvalue to smallest eigenvalue,

$$\gamma = \frac{\lambda_{\max}}{\lambda_{\min}}. \quad (10)$$

As an example, consider a 240 sample Hamming window and 10'th order LP analysis. The input speech is modified IRS filtered [3] and sampled at 8 kHz. The condition number of the autocorrelation matrix and the maximum predictor coefficient values were measured across a data

base of 25 speakers, including two children, for a total of 224,779 frames. Figure 1 shows a histogram of the condition number expressed in power dB. The largest condition number encountered was 56.4 dB. The largest predictor coefficient generated was 11.0 for a frame with a condition number of 48.7 dB. These frames occur during normal speech. For instance, the frame with the largest condition number occurs in male speech in the middle of the word “both” in the sentence “The pencil was cut sharp at both ends”. The largest predictor coefficient occurs in female speech at the end of the word “floor” in the sentence “Tack the strip of carpet to the worn floor”. In both cases, the waveforms in these regions are somewhat sinusoidal.

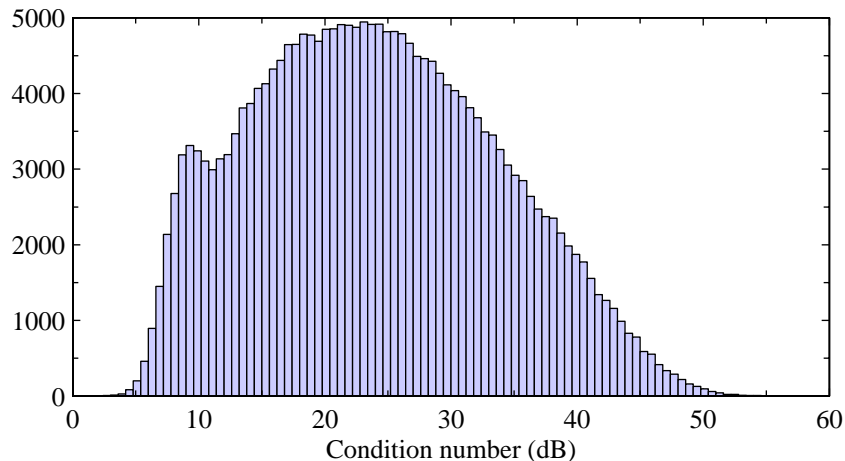


**Fig. 1** Histogram of condition numbers (dB).

Figure 2 shows a scatter plot of the values of the largest predictor value<sup>1</sup> against the condition number for each frame in the database. There are only a few frames with large predictor values (exceeding  $\pm 8$ ) and they tend to occur for large condition numbers.

## 2.2 Power Spectrum Modification

The eigenvalues of a Toeplitz matrix formed from autocorrelation values are bounded by the minimum and maximum values of the power spectrum [6, 8]

$$\lambda_{\max} \leq \max_{\omega} S(\omega), \quad \lambda_{\min} \geq \min_{\omega} S(\omega), \quad (11)$$

$$\gamma = \frac{\lambda_{\max}}{\lambda_{\min}} \leq \frac{\max_{\omega} S(\omega)}{\min_{\omega} S(\omega)}, \quad (12)$$

---

<sup>1</sup>The largest predictor value can take on either sign.

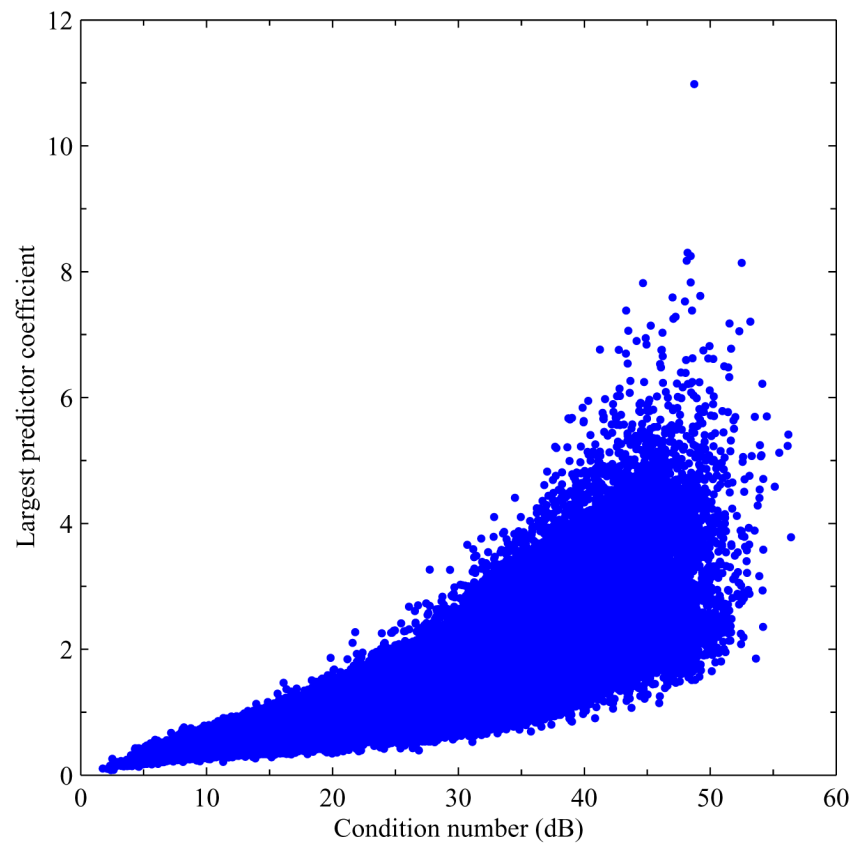


**Fig. 2** Scatter plot of the largest predictor value and the condition number for each frame in the database.

where the power spectrum is the Fourier transform of the correlation values and is given by

$$S(\omega) = \sum_{k=-\infty}^{\infty} r[k] e^{j\omega k}. \quad (13)$$

Note that this sum involves all of the autocorrelation coefficients, not just those that appear in the correlation matrix. The condition number is related to the fluctuations in the power spectrum — a flat spectrum gives the best conditioned equations, while spectra with large dynamic ranges can give badly conditioned equations.

Consider spectra with large peaks. These can be due to sinusoidal components, for instance dual (DTMF) tones used for signalling. They can, however, also occur in speech. A high pitched voice (female or child) uttering a nasalized sound can generate a surprisingly sinusoidal waveform. Problems occur because these sinusoidal components are very predictable. In fact for pure sines, only two predictor coefficients per sinusoid are needed to achieve perfect prediction. After applying a tapered window to the input data, we no longer have a pure sinusoids, but the effect of ill-conditioning is still present. As we saw earlier, large condition numbers occur for segments of ordinary speech.

### 2.2.1 Diagonal loading

A simple modification to reduce the eigenvalue spread is diagonal loading of the correlation matrix (adding a positive term to the zeroth autocorrelation coefficient).<sup>2</sup> In the power spectral domain, this is equivalent to adding a constant white noise term (referred to as white noise compensation). The compensation reduces the bound on the eigenvalue spread.

This same approach is used in fractional spacing equalizers for data transmission [5]. There the problem is ill-conditioning due to over-sampling. Adaptive adjustment algorithms such as LMS are subject to having the taps wander into overload regions. The mean-square error criterion can be modified to constrain the size of the predictor coefficients,

$$\varepsilon' = \varepsilon + \mu \mathbf{p}^T \mathbf{p}. \quad (14)$$

Taking the derivative with respect to the tap weights gives equations of the same form as earlier, but with the correlation matrix replaced by

$$\mathbf{R}' = \mathbf{R} + \mu \mathbf{I}. \quad (15)$$

---

<sup>2</sup>In the matrix computations literature a similar approach is termed *ridge regression* [7].

For our case of Toeplitz correlation matrices, we can write the modified correlation values as

$$r'[k] = r[k] + \mu\delta[k]. \quad (16)$$

We will make  $\mu$  proportional to  $r[0]$ ,

$$\mu = \epsilon r[0], \quad (17)$$

giving a multiplicative modification of the correlations

$$r'[k] = r[k](1 + \epsilon\delta[k]). \quad (18)$$

With the modified correlation, the bounds on the condition number ( $\epsilon \geq 0$ ) are as follows,

$$\gamma \leq \frac{\max_{\omega} (S(\omega) + \epsilon r[0])}{\min_{\omega} (S(\omega) + \epsilon r[0])} \leq \frac{\max_{\omega} S(\omega)}{\min_{\omega} S(\omega)}. \quad (19)$$

Applying diagonal loading by multiplying the zeroth correlation value by the factor 1.0001 ( $\epsilon = 0.0001$ ) improves the condition numbers. The largest condition number is now 48 dB and the largest predictor value is now 4.6 (within the range of  $\pm 8$  for Q12 representation). A histogram of the resulting condition numbers is shown in Fig. 3.

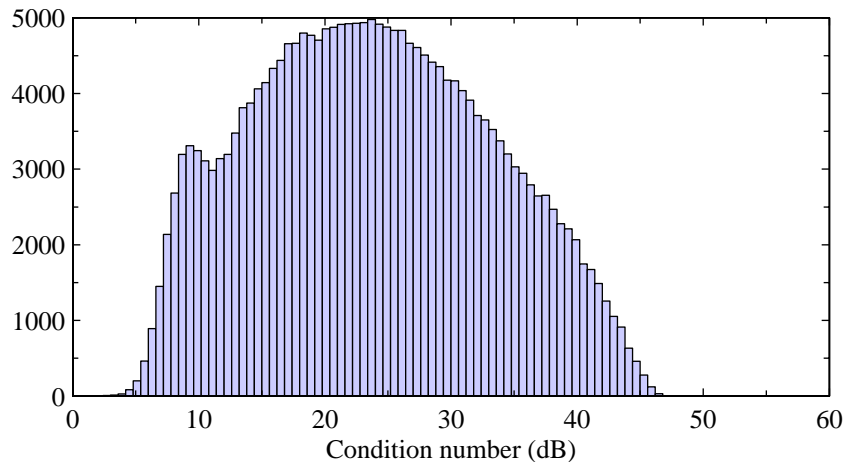


**Fig. 3** Histogram of condition numbers (dB), white noise compensation with  $\epsilon = 0.0001$ .

The use of white noise compensation comes at the loss of optimality of the predictor for all frames. We can measure the predictor performance in terms of the ratio of the energy of the input

signal to the energy of the prediction residual  $\varepsilon$  (see Eq. (7)). Specifically, the prediction gain is

$$G_P = \frac{r[0]}{\varepsilon}. \tag{20}$$

A histogram of the original prediction gains (in dB) (i.e., without white noise compensation) is shown in Fig. 4. A plot of the loss in prediction gain due to white noise compensation ( $\epsilon = 0.0001$ ) is shown in Fig. 5. This is measured with the predictor coefficients calculated with white noise compensation acting on the original windowed input. The plot has points corresponding to the bins of the histogram of prediction gains. For each point, the circle indicates the average of the losses in prediction gains (in dB) within the histogram bin. The error bars indicate the smallest and largest prediction gain losses within the bin. One can notice that for frames with prediction gains below about 27 dB, the average prediction gain loss due to the use of white noise compensation (circles on the plot) is near the minimum loss. This indicates that the larger losses in prediction gain are rare. For the frames with higher prediction gains, the mean loss in prediction gain lies close to midway between the minimum and maximum values.

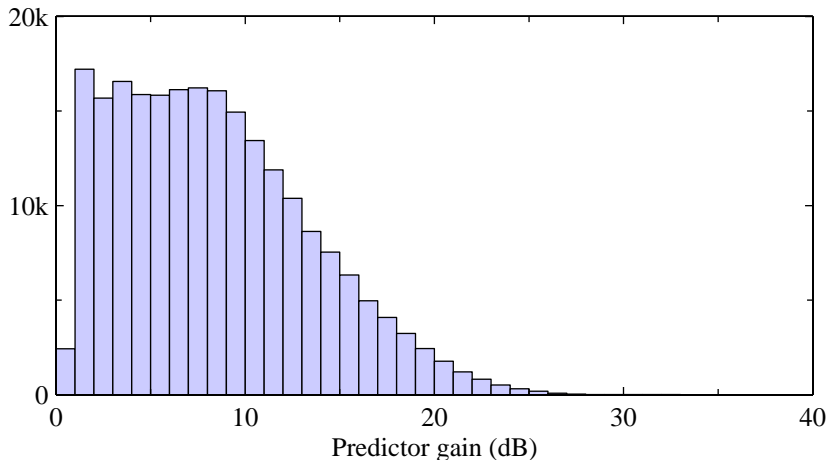


**Fig. 4** Histogram of the prediction gains.

The effect of changing  $\epsilon$  was tested across the database. Figure 6 shows the maximum condition number as a function of the amount of white noise compensation. The curve is relatively smooth in spite of the fact that the speech frame giving the largest condition number is not the same for the different points on the plot. Figure 7 shows the largest predictor coefficient value as a function of the amount of white noise compensation. It can be seen that the choice of  $\epsilon = 0.0001$  is a reasonable value to keep the largest predictor coefficient below 8.

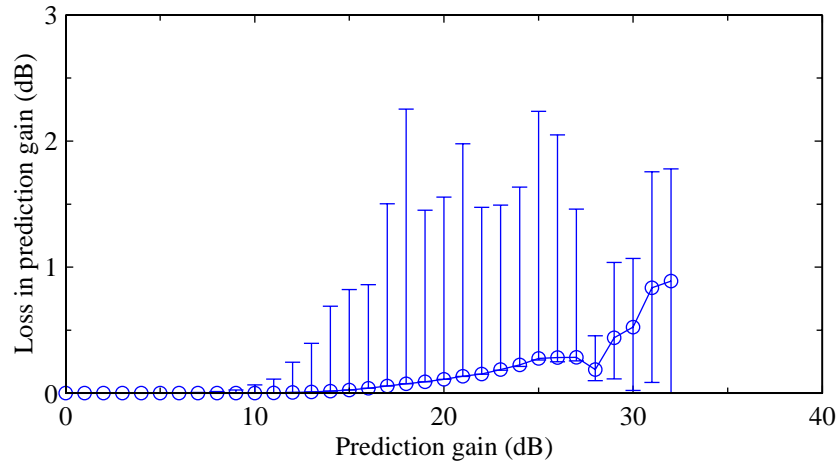


**Fig. 5** Loss in prediction gain due to white noise compensation ( $\epsilon = 0.0001$ ) versus the original prediction gain. The circles indicate the average of the prediction gain losses (in dB), while the error bars indicate the minimum and maximum prediction gain losses.

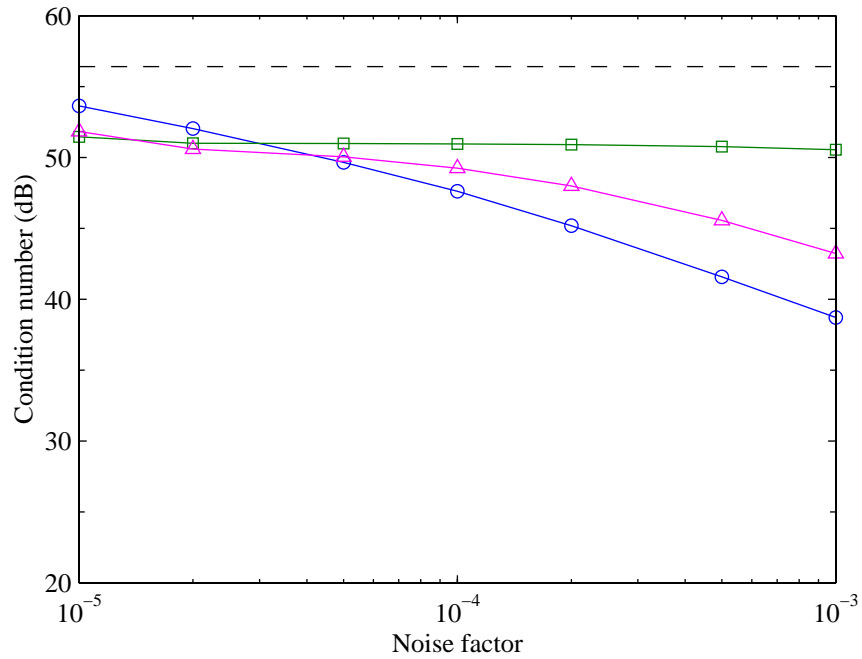


**Fig. 6** Largest condition number versus  $\epsilon$  (circles: white noise compensation, squares: highpass noise compensation, triangles: mixed noise compensation). The dashed line is the largest condition number for  $\epsilon = 0$ .

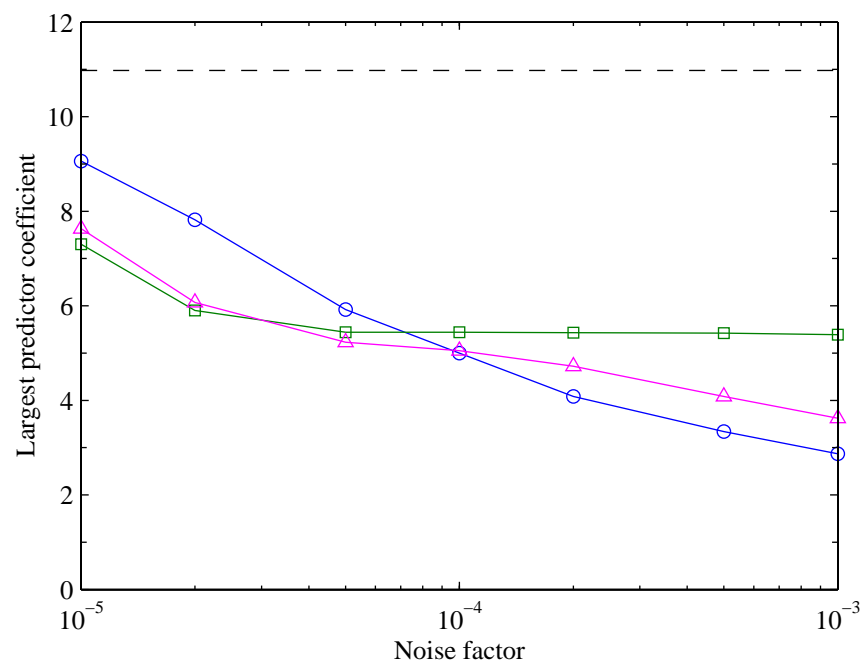


**Fig. 7** Largest predictor coefficient value versus  $\epsilon$  (circles: white noise compensation, squares: highpass noise compensation, triangles: mixed noise compensation). The dashed line is the largest predictor coefficient value for  $\epsilon = 0$ .

### 2.2.2 High frequency compensation

A slightly different tack to improve conditioning was taken by Atal and Schroeder [9]. Their concern was that a large power gain (sum of the squares of the predictor filter coefficients) causes excessive feedback of quantization noise in a closed loop quantizer. They identified that the ill-conditioning that leads to large power gains was caused by the use of sharp lowpass filters in the signal path. These filters tend to leave a null in the spectrum near the half-sampling frequency. To compensate for this spectrum null, they applied a high-frequency compensation by adding the correlation for highpass noise to the speech correlation matrix.

The noise spectrum used in [9] was that of white noise filtered by a highpass filter,

$$H_{\text{HP}}(z) = (1 - z^{-1})^2. \quad (21)$$

For input white noise, the correlation function for the output highpass noise, normalized to unit variance, is

$$r_n[k] = \begin{cases} 1 & \text{for } k = 0, \\ -\frac{2}{3} & \text{for } |k| = 1, \\ \frac{1}{6} & \text{for } |k| = 2, \\ 0 & \text{elsewhere.} \end{cases} \quad (22)$$

The power spectrum of the highpass noise has a peak value  $8/3$  times that for white noise of the same power. The peak occurs at  $\omega = \pi$ , while a null occurs at  $\omega = 0$ .

This correlation for the highpass noise will be added to the signal correlation,

$$r'[k] = r[k] + \epsilon r[0] r_n[k]. \quad (23)$$

A histogram of the condition numbers for highpass noise compensation ( $\epsilon = 0.0001$ ) is shown in Fig. 8. Note that the histogram falls off dramatically above 40 dB, but a small number of frames still have condition numbers which reach up to 51 dB (see Fig. 6). The present histogram for highpass noise compensation can be compared to the previous histogram for white noise compensation of the same energy (see Fig. 3).

The effect of varying  $\epsilon$  on the largest predictor coefficient value is shown as one of the curves in Fig. 7. One can see that for small values of  $\epsilon$ , highpass noise is more effective at reducing the maximum coefficient value than white noise of the same energy. When  $\epsilon$  is large, the predictor coefficients will be those appropriate for predicting the highpass noise. The largest predictor coefficient for this case is 2.18. This is in contrast to the white noise compensation situation, in which the predictor coefficients move towards zero as  $\epsilon$  increases.

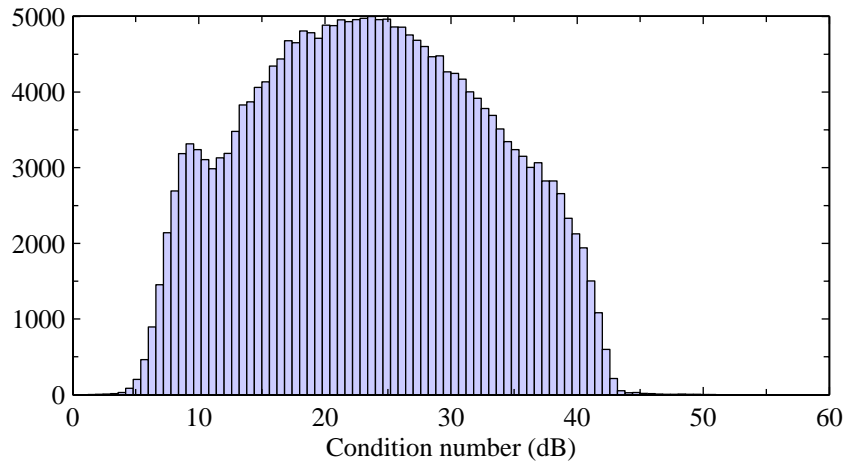


**Fig. 8** Histogram of condition numbers (dB), highpass noise compensation with  $\epsilon = 0.0001$ .

A mixed form of noise compensation was also tried. The mixed noise combines white noise and highpass noise, with the portions adjusted to control the ratio of the power spectrum at zero frequency to the power spectrum at  $\pi$ . This ratio was chosen to be  $1/10$ . The noise has a highpass nature, but a significant amount of noise remains at low frequencies. The resulting noise correlation values (unit variance) are

$$r_n[k] = \begin{cases} 1 & \text{for } k = 0, \\ -\frac{18}{35} & \text{for } |k| = 1, \\ \frac{9}{70} & \text{for } |k| = 2, \\ 0 & \text{elsewhere.} \end{cases} \quad (24)$$

The modified correlation is obtained by adding the scaled highpass correlation to the signal correlation,

$$r'[k] = r[k] + \epsilon r[0] r_n[k]. \quad (25)$$

The effect of varying  $\epsilon$  on the condition number and on the maximum predictor coefficient value is shown in Fig. 6 and Fig. 7. The mixed noise is marginally preferable (over white noise) for small values of  $\epsilon$ . It was initially hoped that for a given value of  $\epsilon$ , the prediction gain loss for mixed noise would be less than the loss for white noise. This did not turn out to be so. The average prediction loss, for instance at  $\epsilon = 0.0001$ , was significantly larger than that for white noise compensation.

### 2.2.3 Selective power spectrum compensation

The previous approaches bias the solutions even when the equations are already well conditioned. Instead of adding a constant power spectrum (white noise compensation), an approach which fills in only spectral valleys will be tested,

$$S'(\omega) = \max(S(\omega), \epsilon r[0]), \tag{26}$$

where  $\epsilon r[0]$  is the power spectrum of the white noise. This approach modifies only those regions of the power spectrum of the signal that fall below that of the white noise. This process can be viewed as adding a noise correlation tailored to fill in the spectral valleys.

In practice, we have to use a DFT (via an FFT) which only gives us samples of the spectrum. Nonetheless, this process can be approximated as follows.

1. Compute the energy of the frame ( $r[0]$ ).
2. Pad the data frame to at least twice its length with zeros to avoid time aliasing. If the length of the frame is  $N_f$ , a vector of length at least  $2N_f - 1$  is needed.
3. Take the DFT of the vector of samples.
4. Calculate the square magnitude of the frequency response to get the power spectrum.
5. Replace all values of the power spectrum falling below  $\epsilon r[0]$  with that value.
6. Take the inverse DFT of the modified power spectrum. The first  $N_p + 1$  values of the resulting correlation values will be used in the correlation equations.

This approach was implemented and the value of  $\epsilon$  was varied. For a given value of  $\epsilon$ , with selective power spectrum modification, the power spectrum is modified less than for the white noise case. The bounds on the condition number ( $\epsilon \geq 0$ ) are as follows,

$$\gamma \leq \frac{\max_{\omega} S(\omega)}{\min_{\omega} \max(S(\omega), \epsilon r[0])} \leq \frac{\max_{\omega} S(\omega)}{\min_{\omega} S(\omega)}. \tag{27}$$

Depending on the value of  $\epsilon$ , the bound for selective power spectrum modification can be smaller or larger than the bound for white noise compensation (see Eq. (19)). Experiments show that the maximum condition number for the white noise case is smaller than the maximum condition number for the selective power spectrum modification case. If the maximum condition number versus  $\epsilon$  curve is compared to the curve of white noise compensation (as in Fig. 6) it appears appear slightly above (about 1 dB at  $\epsilon = 0.0001$ ) and nearly parallel to the white noise curve.

With  $\epsilon = 0.0001$ , the selective power spectrum modification approach changes the spectrum in 91% of the frames. The condition number for selective power spectrum compensation for  $\epsilon = 0.0001$  is very close to that for white noise compensation with  $\epsilon$  about 20% smaller. For those respective values of  $\epsilon$ , the plots of the loss of prediction gain due to the modification of the correlation are very similar (see Fig. 5 for the white noise case). Given the similar results, the extra computation that is entailed by the selective power spectrum modification is hard to justify with respect to simple white noise compensation.

White noise compensation directly controls the sum of the squares of the prediction coefficient values. As such, it also tends to control the maximum prediction coefficient value. The other methods considered also affect the maximum prediction coefficient values, but in a more indirect way.

In a later section, we consider lag windowing applied to the correlation values. This strategy is usually motivated by the need for bandwidth expansion. It does however have an effect on the conditioning of the LP equations.

#### 2.2.4 Notes on the addition of noise correlation

The optimization problem with the addition of noise can be written as

$$\varepsilon' = r[0] - 2\mathbf{p}^T \mathbf{r} + \mathbf{p}^T \mathbf{R} \mathbf{p} + \mu(r_n[0] - 2\mathbf{p}^T \mathbf{r}_n + \mathbf{p}^T \mathbf{R}_n \mathbf{p}). \quad (28)$$

The predictor coefficients which minimize  $\varepsilon'$  are found from

$$(\mathbf{R} + \mu \mathbf{R}_n) \mathbf{p} = \mathbf{r} + \mu \mathbf{r}_n. \quad (29)$$

For  $\mu = 0$ , we get the unmodified solution. For large  $\mu$ , we get the predictor coefficients for prediction of the noise. Note that  $\mathbf{r}_n$  is zero for white noise, but is non-zero for coloured noise.

An alternate minimization problem is

$$\varepsilon' = r[0] - 2\mathbf{p}^T \mathbf{r} + \mathbf{p}^T \mathbf{R} \mathbf{p} + \mu \mathbf{p}^T \mathbf{R}_n \mathbf{p}. \quad (30)$$

With this formulation, the predictor coefficients to minimize  $\varepsilon'$  are found from

$$(\mathbf{R} + \mu \mathbf{R}_n) \mathbf{p} = \mathbf{r}. \quad (31)$$

As  $\mu$  gets large the predictor coefficients go to zero.

In both formulations the effective correlation matrix is Toeplitz. However, for the second case, the right-hand vector does not include the same correlation elements as the matrix. If one

distinguishes the solution methods of Levinson (arbitrary right-hand vector) and Durbin (right-hand vector drawn from the matrix elements), the first formulation can use the Durbin recursion, while in the second the Levinson method must be used. In addition to the (modest) increase in computational complexity for the second formulation, one can no longer guarantee that the prediction error filter coefficients are minimum phase. It is only for the white noise case that the two formulations coincide.

### 2.3 Correction in the Levinson-Durbin Recursion

Correction can be applied while solving the correlation equations. We will examine the use of trigger parameters that are the by-product of a standard Levinson-Durbin recursion, and hence do not impose a significant additional computational overhead.

#### 2.3.1 Limiting the prediction gain

In the Durbin recursion, the residual energy is available at each iteration. It is easy to modify the procedure to test the prediction gain (ratio of residual energy to initial energy) at each iteration. If the maximum prediction gain is exceeded, the iterations are terminated, keeping the previously calculated predictor values and setting remaining prediction coefficients to zero. All frames with (final) prediction gains below the threshold are unchanged.

This procedure described in the previous paragraph was implemented. A limit of about 17 dB on the prediction gain brings the largest coefficient value below 8. With this threshold, the iterations were prematurely terminated in about 6.5% of the frames. Further insight can be gained from a scatter plot of the largest predictor coefficient versus the prediction gain (see Fig. 9). The results show that large coefficient values can occur for frames with only moderately high prediction gains. In fact it shows that the largest prediction value across all frames occurs for a frame with a prediction gain of about 18 dB.

#### 2.3.2 Limiting the largest reflection coefficient

Reflection coefficients with magnitude near unity signal ill-conditioning. At stage  $k$  in the Durbin recursion, the last coefficient of the predictor coefficients is equal to the  $k$ th reflection coefficient. But, the last predictor coefficient is the product of the roots. If all of the roots are near unity, the reflection coefficient will also have a magnitude near unity.

We can terminate the Durbin recursion when the absolute value of a reflection coefficient exceeds a threshold value. The predictor coefficients from the previous iteration will be retained. This procedure was implemented, but the threshold on the reflection coefficient necessary to bring the largest prediction coefficient value below 8 was much too aggressive. With a threshold of 0.75

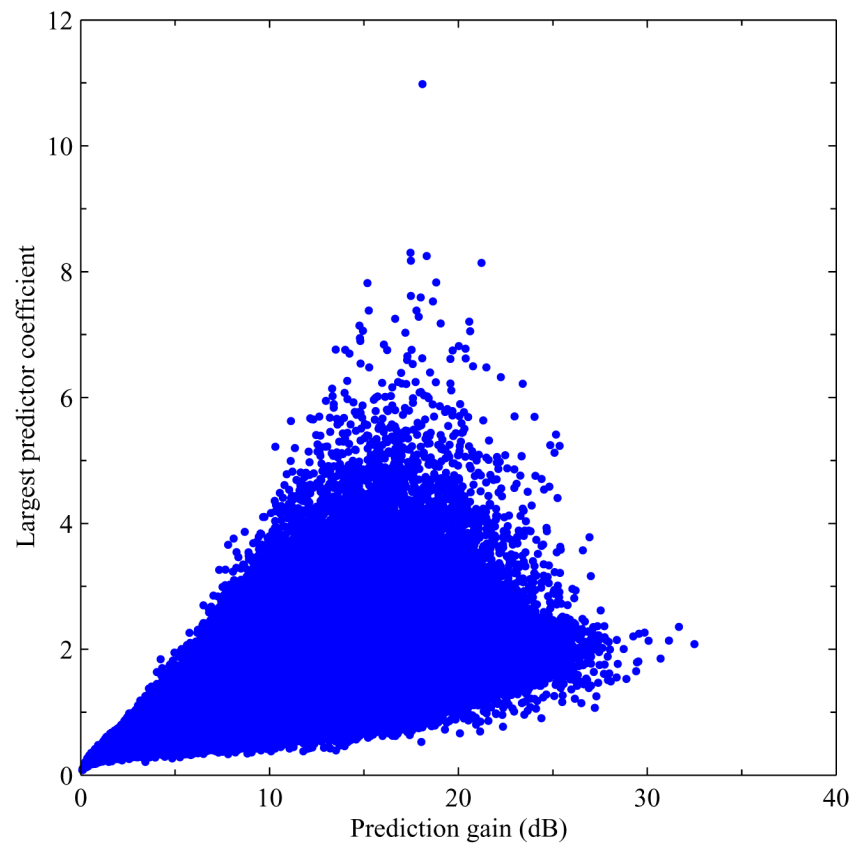


**Fig. 9** Scatter plot of the largest predictor value and the prediction gain for each frame in the database.

on the reflection coefficient, 23% of the frames are affected. At such a setting, the large loss in prediction gain is unacceptable. A scatter plot of the largest predictor value against the largest reflection coefficient shows that large predictor coefficients can occur for relatively small reflection coefficient values (see Fig. 10).

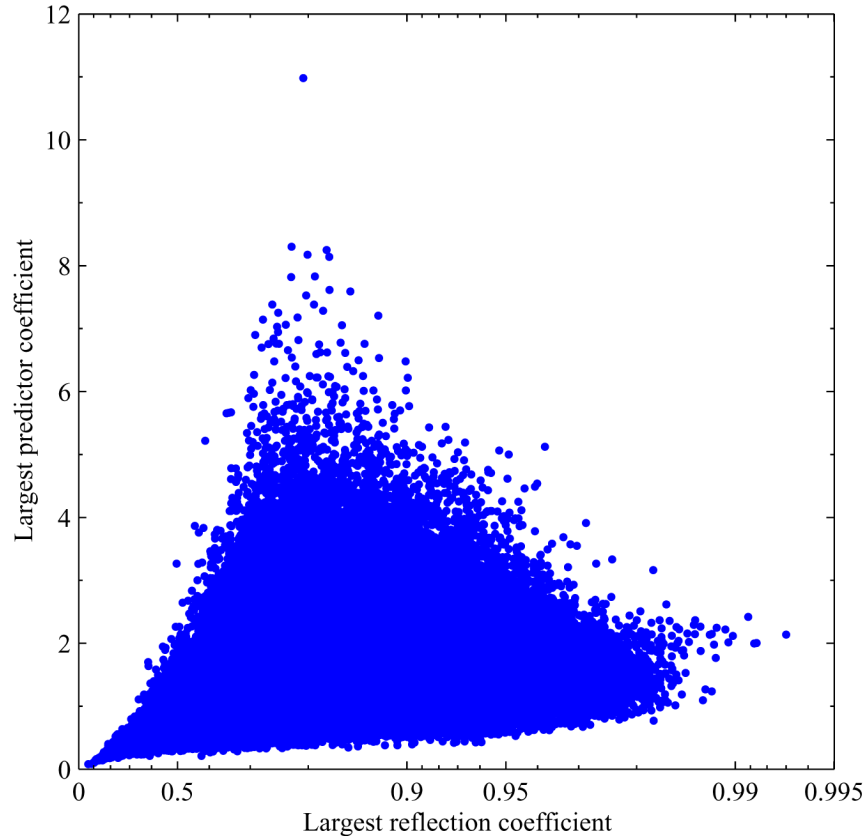


**Fig. 10** Scatter plot of the largest predictor value and the largest reflection coefficient for each frame in the database.

### 3 Bandwidth Expansion

Bandwidth expansion is the process of taking a frequency response, usually with resonances or peaks, and broadening the bandwidths of those peaks. Such an expansion is useful in speech processing to prevent unnatural spectral peaks due to formant/pitch interactions. Such bandwidth expansion can be implemented before LP analysis (time windows or lag windowing) or on the LP coefficients after LP analysis (spectral damping).

### 3.1 Bandwidth Expansion Before LP Analysis

Bandwidth expansion before LP analysis can serve its purpose of broadening spectral peaks, but since it is done before LP analysis, it will also affect the conditioning of LP equations.

#### 3.1.1 Time windows

The input signal is usually windowed with a tapered window (Hamming or other) prior to calculating the correlation values. The effect of the window can be described in the frequency domain as a convolution of the frequency response of the window with the frequency response of the signal. This in itself constitutes a form of implicit bandwidth expansion since the window response has a non-zero main lobe width. For instance, the main lobe width (measured between zero crossings) for a Hamming window is  $8\pi/N$  (asymptotically in  $N$ ), where  $N$  is the window length. The 3 dB width of the main lobe is 65% of this value. For a 240 sample Hamming window (8 kHz sampling), the main lobe width of the frequency response of the Hamming window is 135 Hz between zero crossings and 44 Hz at the 3 dB points. Some bandwidth expansion due to time windowing is unavoidable, since the narrowest main lobe (for a rectangular time window) is 1/2 of the value for a Hamming window of the same length.

#### 3.1.2 Correlation windowing

Explicit bandwidth expansion prior to LP analysis is done by lag windowing the autocorrelation sequence [10, 11], often with a Gaussian or binomial shaped window. Since the autocorrelation sequence has as its Fourier transform the power spectrum, this correlation windowing corresponds to a periodic convolution of the frequency response of the window with the power spectrum. With lag windowing, a narrow spectral line will take on the shape of the window spectrum.

Consider a Gaussian window which is a function of continuous time,

$$w(t) = \exp\left(-\frac{1}{2}(at)^2\right). \quad (32)$$

The frequency response of this window also has a Gaussian shape,

$$W(\Omega) = \frac{\sqrt{2\pi}}{a} \exp\left(-\frac{1}{2}\left(\frac{\Omega}{a}\right)^2\right). \quad (33)$$

The two-sided bandwidth (radians) measured between the 1 standard deviation points for this curve is  $2a$ . From the form of the Gaussian curve, the two-sided 3 dB bandwidth is  $\omega_{\text{bw}} = \sqrt{8\log(2)}a$ , i.e., the 3 dB bandwidth is about 18% larger than the 1- $\sigma$  bandwidth.

In fact the window is applied in discrete-time leading to frequency aliasing of the Gaussian

frequency response. However with reasonably chosen bandwidth expansion factors and given the fact that the Gaussian frequency response dies off quickly, the effect of aliasing can be largely ignored in the calculation of the effective bandwidth expansion. The discrete-time window is

$$w[k] = \exp\left(-\frac{1}{2}\left(\frac{ak}{F_s}\right)^2\right), \quad (34)$$

where  $F_s$  is the sampling rate. The parameter  $a$  can be expressed in terms of  $F_{\text{bw}}$ , the two-sided  $1\text{-}\sigma$  bandwidth in Hz,

$$a = \pi F_{\text{bw}}/F_s. \quad (35)$$

Lag windowing also affects the conditioning of the LP equations. Spreading the spectrum has the effect of helping to fill in spectral valleys and hence potentially reducing the condition number of the correlation matrix. In fact, this effect on conditioning is given as one rationale for using the lag window [4]. The ITU-T G.729 8 kb/s CS-ACELP [1] and SMV [2] speech coders use a bandwidth  $F_{\text{bw}} = 120$  Hz (referred to as a bandwidth of 60 Hz in the coder standards) relative to a sampling rate  $F_s = 8000$  Hz. Tests were run with the G.729/SMV lag window. Surprisingly, the effect of the worst condition number is small (now 56.0 dB, only a little better than the original 56.4 dB). Also the largest predictor coefficient value is now 10.7, only a little smaller than the original value of 11.0.

The above indicates that lag windowing with a Gaussian window by itself does not improve the conditioning by much. However, white noise compensation can be represented as a lag window (see Eq. (18)). In fact, lag windowing and white noise compensation can be combined into a single lag window. The combined effect of lag windowing (120 Hz bandwidth) and white noise compensation ( $\epsilon = 0.0001$ ) on the prediction gain is shown in Fig. 11. The figure can be compared to Fig. 5 which gives the situation for no lag windowing. One can note that the use of lag windowing causes additional loss of prediction gain, especially for frames with prediction gains below about 15 dB.

### 3.2 Bandwidth Expansion After LP Analysis

In this section, we investigate bandwidth expansion after LP analysis. Consider a digital filter  $H(z)$  and a bandwidth expanded version of this filter. In many cases, it is important that the bandwidth expanded version of the filter have the same form. For instance if  $H(z)$  is an all-pole filter (as would arise from a standard LP analysis), the bandwidth-expanded version should also be all-pole.

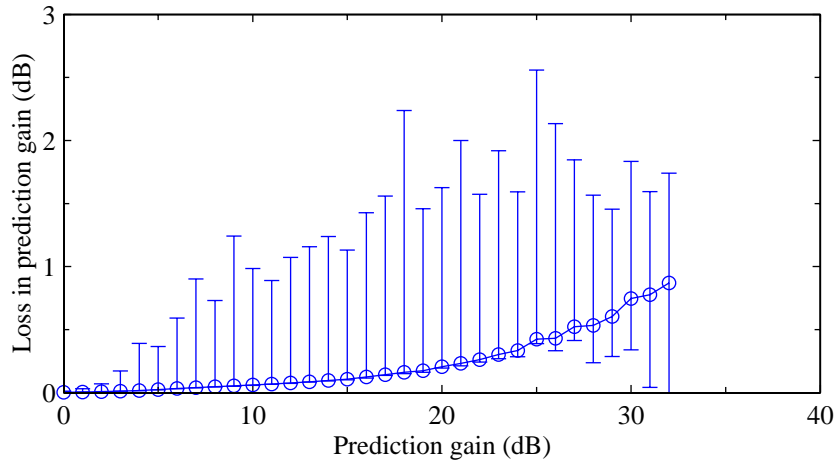


**Fig. 11** Loss in prediction gain due to lag windowing (120 Hz bandwidth) and white noise compensation ( $\epsilon = 0.0001$ ) versus the original prediction gain. The circles indicate the average of the prediction gain losses (in dB), while the error bars indicate the minimum and maximum prediction gain losses.

Replacing  $z$  by  $z/\alpha$  satisfies this requirement. Consider the all-pole filter,

$$H(z) = \frac{1}{A(z)} = \frac{1}{1 - \sum_{k=1}^N p_k z^{-k}}.$$

With bandwidth expansion [12], the filter has the same form, but with a new set of coefficients,

$$p'_k = \alpha^k p_k.$$

Replacing  $z$  by  $z/\alpha$  moves the singularities of  $H(z)$  inward ( $\alpha < 1$ ) or outward ( $\alpha > 1$ ). For a filter with resonances, choosing  $\alpha < 1$  has the effect of expanding the bandwidth of the resonances.

### 3.2.1 Windowing with an exponential sequence

For a causal filter, the effect of replacing  $H(z)$  with  $H(z/\alpha)$  is such that the impulse response of the filter is modified to become

$$h'[n] = \alpha^n h[n], \quad (36)$$

i.e., the impulse response coefficients are multiplied by an exponential (infinite length) time window. In the frequency domain, the frequency response of the filter is convolved with the frequency

response of the window,

$$W(\omega) = \frac{1}{1 - \alpha e^{-j\omega}}. \quad (37)$$

The 3 dB bandwidth of the window frequency response is

$$\omega_{\text{bw}} = 2 \cos^{-1} \left( 1 - \frac{(1 - \alpha)^2}{2\alpha} \right) \quad \text{for } 3 - 2\sqrt{2} \leq \alpha \leq 1. \quad (38)$$

Below the lower limit for  $\alpha$ , the response does not decrease sufficiently to fall 3 dB below the peak.

### 3.2.2 Radial scaling of a bandpass filter

To see the effect of replacing  $z$  by  $z/\alpha$  from another point of view, consider a bandpass filter with a single resonance. The bandwidth of a resonance has been well studied for continuous-time systems. We will find the discrete-time bandpass filter related to it through a bilinear transformation.

#### *Continuous-time bandpass filter*

The second-order bandpass filter is

$$H(s) = \frac{s}{s^2 + (\Omega_o/Q)s + \Omega_o^2}. \quad (39)$$

Assume that  $\Omega_o > 0$  and  $Q > 0$ . The frequency response for this filter has a peak at  $\Omega_o$ . The 3 dB points of the response have a simple relation that is developed in Appendix A,

$$\Omega_u - \Omega_l = \Omega_o/Q. \quad (40)$$

Note that the frequency response exhibits a resonance even when the poles are real ( $Q \leq 1/2$ ).

#### *Digital bandpass filter*

The corresponding digital filter can be found using a bilinear transformation,

$$z = -\frac{s+a}{s-a}. \quad (41)$$

The parameter  $a$  is real. This transformation maps the zeros at  $s = 0$  and  $s = \infty$  to  $z = +1$  and  $z = -1$ , respectively. For complex poles, the poles get mapped to new locations  $z_{1,2} = r_p e^{\pm j\omega}$ ,

$$H(z) = \frac{z^2 - 1}{z^2 - 2r_p \cos \omega_o z + r_p^2}. \quad (42)$$

Using the bilinear relationship, the 3 dB points in the response can be found for the digital filter. The 3 dB bandwidth has a particularly simple form (see Appendix B),

$$\omega_{\text{bw}} = \pi/2 - 2 \tan^{-1}(r_1 r_2). \tag{43}$$

where  $r_1$  and  $r_2$  are the radii of the poles of the digital filter. Note that the poles do not have to be complex for this equation to apply, although our main interest is the case of resonances for which the poles are complex conjugates and  $r_1 = r_2$ .

*Bandwidth expansion*

Consider scaling the  $z$ -transform

$$H'(z) = H(z/\alpha), \tag{44}$$

where  $0 < \alpha \leq 1$ . Then the new poles have radii  $r'_1 = \alpha r_1$  and  $r'_2 = \alpha r_2$ . The 3 dB bandwidth of the resonance is now

$$\omega'_u - \omega'_l = \pi/2 - 2 \tan^{-1}(\alpha^2 r_1 r_2). \tag{45}$$

The difference in bandwidth due to radial scaling by  $\alpha$  is

$$\Delta\omega_{\text{bw}} = 2 \tan^{-1}\left(\frac{r_1 r_2 (1 - \alpha^2)}{1 + \alpha^2 r_1^2 r_2^2}\right). \tag{46}$$

This bandwidth expansion given by Eq. (46) is plotted in Fig. 12 for three different values of  $r = r_1 = r_2$ . This figure indicates that the predicted bandwidth expansion only occurs for very sharp resonances. The actual bandwidth expansion for less sharp resonances is significantly smaller.

In the limiting case of poles near the unit circle ( $r_1 = r_2 = 1$ ), the bandwidth after applying a bandwidth expansion factor of  $\alpha$  is

$$\omega_{\text{bw}} = \pi/2 - 2 \tan^{-1}(\alpha^2). \tag{47}$$

**3.2.3 Comparison of bandwidth formulas**

We now have two formulas, Eqs. (38) and (47), which account for the effect of radial scaling of the  $z$ -transform. These give the bandwidth of a narrow spectral line after bandwidth expansion. The bandwidth expressions derived here can be compared to approximations that have appeared in the literature. Paliwal and Kleijn [13] give the bandwidth formula (converted to our notation)

$$\omega_{\text{bw}} = -2 \log(\alpha). \tag{48}$$

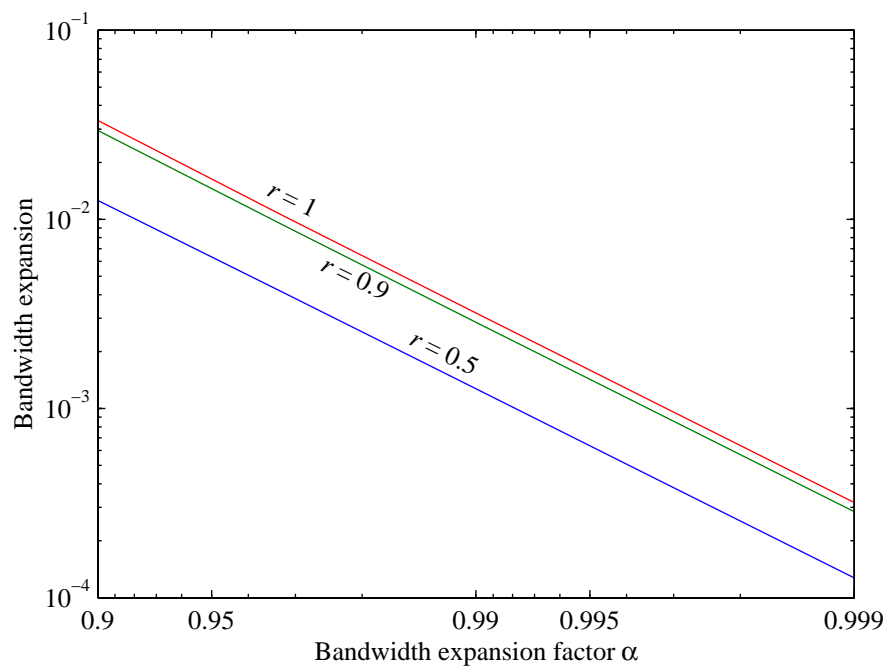


**Fig. 12** Fractional bandwidth expansion ( $\Delta\omega_{\text{bw}}/(2\pi)$ ) as a function of the bandwidth expansion parameter  $\alpha$ .

This formulation can be derived from an impulse invariant transformation of a continuous-time exponential sequence. As such it ignores the aliasing effects that are taken care of in the derivation leading to Eq. (38).

For  $\alpha$  near unity, all three expressions give similar results. An examination of the Taylor series for the three expressions shows that they agree in value and the first derivative at  $\alpha = 1$ ,

$$\omega_{\text{bw}} = 2(1 - \alpha) + (1 - \alpha)^2 + O((1 - \alpha)^3). \tag{49}$$

The bandwidths estimated by the different expressions are plotted in Fig. 13. The ordinate is the bandwidth normalized to the sampling frequency,  $(\omega_{\text{bw}}/(2\pi))$ . On this figure, we also plot a simple estimate of the bandwidth based on the first two terms of the Taylor series,

$$\omega_{\text{bw}} = 2(1 - \alpha) + (1 - \alpha)^2. \tag{50}$$

The figure shows that this formula gives a good estimate of the bandwidth for useful values of  $\alpha$ . Based on the simple bandwidth formula, we can find  $\alpha$  for a given bandwidth,

$$\alpha = 2 - \sqrt{1 + 2\pi F_{\text{bw}}/F_s}, \tag{51}$$

where  $F_{\text{bw}}$  is the 3 dB bandwidth in Hz and  $F_s$  is the sampling frequency.

In speech coding, bandwidth expansion with bandwidth values of 10 Hz to 25 Hz is used. With a sampling rate of 8000 Hz, these bandwidths correspond to values of  $\alpha$  of 0.996 and 0.990. Figure 14 shows the prediction gain loss due to bandwidth expansion using  $\alpha = 0.99$ . The loss in prediction gain is much less than for the lag windowing considered earlier, but so is the amount of bandwidth expansion.

### 3.3 Line Spectral Frequencies

Line spectral frequencies (LSF's) are a transformation of the LP coefficients. The LSF's are an ordered set of values in the range  $(0, \pi)$ . Closely spaced LSF's tend to indicate a spectral resonance at the corresponding frequency. Several standard coders impose minimum separation constraints on the LSF's. This constraint implies a bandwidth expansion that is only applied in exceptional cases.

Another bandwidth expansion scheme for LSF's, albeit for use as a postfilter for speech processing, is described in [14]. In that paper, the LSF's are pushed apart by interpolating the given LSF's with a set corresponding to a flat spectrum (equally spaced LSF's),

$$\omega'[i] = (1 - \mu)\omega[i] + \mu\omega_u[i], \quad i = 1, \dots, N_p, \tag{52}$$

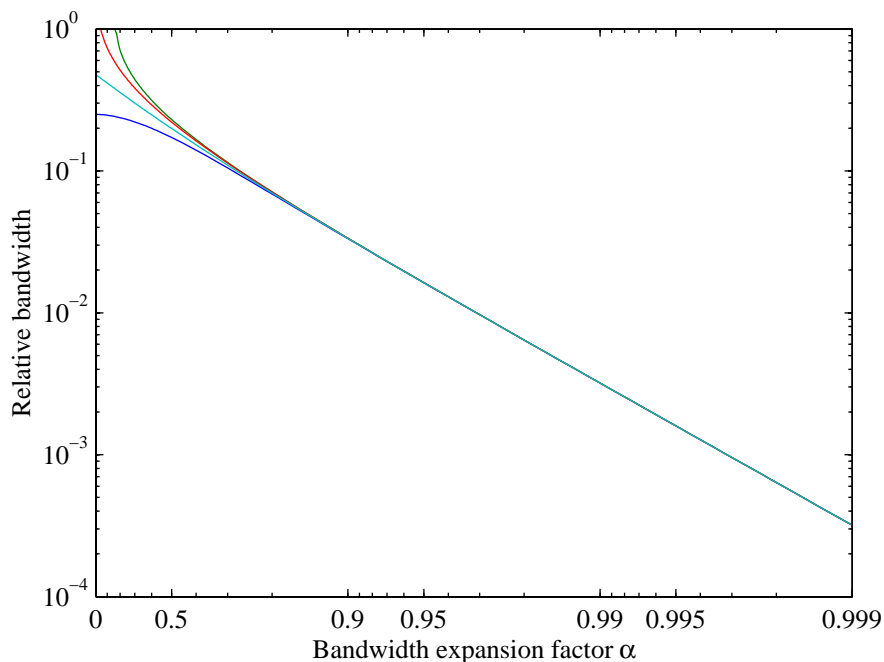


**Fig. 13** Relative bandwidth  $\omega_{bw}/(2\pi)$  as a function of the bandwidth expansion parameter  $\alpha$ . From bottom to top, the curves are the different estimates of  $\omega_{bw}$ :  $\pi/2 - 2 \tan^{-1}(\alpha^2)$ ,  $2(1 - \alpha) + (1 - \alpha)^2$ ,  $-2 \log(\alpha)$ , and  $2 \cos^{-1}(1 - (1 - \alpha)^2/(2\alpha))$ .

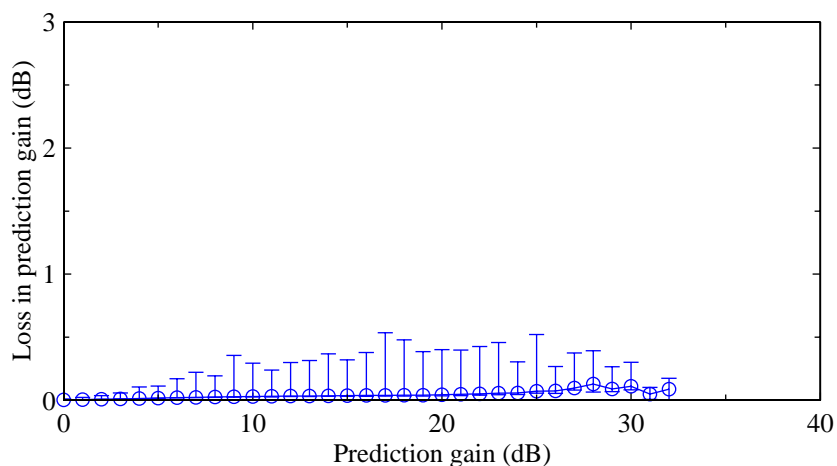


**Fig. 14** Loss in prediction gain due to bandwidth expansion of the predictor coefficients ( $\alpha = 0.99$ ) versus the original prediction gain. The circles indicate the average of the prediction gain losses (in dB), while the error bars indicate the minimum and maximum prediction gain losses.

where  $\omega_u[i] = i\pi/(N_p + 1)$  are the LSF's corresponding to a flat spectrum. Reference [14] also suggests that the target LSF vector  $(\omega_u[i])$  can be generalized, as can the value  $\mu$  by making it a function of frequency.

We will investigate the relationship between LSF separation and the bandwidth of a resonance. Consider a two pole resonance at frequency  $\omega_o$  and radius  $r$  near unity.

$$A(z) = 1 + 2r \cos(\omega_o)z^{-1} + r^2z^{-2}. \quad (53)$$

The LSF's of this error prediction filter (extended with zeros to  $N_p + 1$  terms) are calculated. For most values of  $\omega_o$ , two of the LSF's are closely spaced near  $\omega_o$ . The remaining LSF's are equally spaced from 0 to  $\pi$ . However, the situation is more complicated when  $\omega_o$  approaches one of the equally spaced values. At these points, 3 LSF's play a role in defining the resonance. This situation is illustrated in Fig. 15 for  $N_p = 10$ ,  $r = 0.97$  and sampling frequency 8000 Hz.

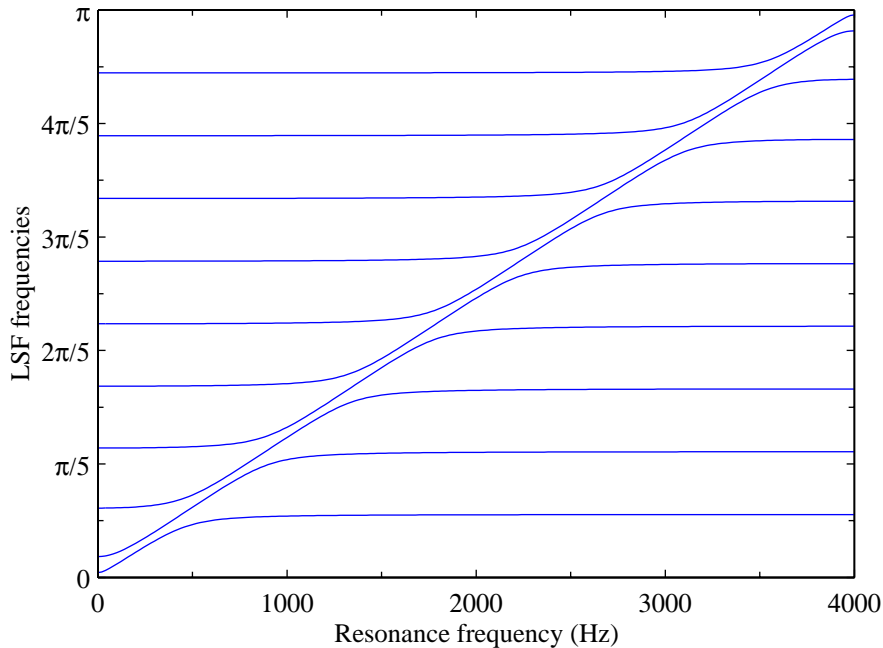


**Fig. 15** LSF values for a resonant system ( $r = 0.97$ ).

The effective bandwidth expansion was investigated for the same resonant system. The resonance is now given a much narrower bandwidth by setting  $r = 0.999$ . The bandwidth expansion formula Eq. (52) is applied to the LSF's using  $\mu = 0.15$ . The bandwidth-expanded LSF's are converted back to give the coefficients of a prediction error filter  $A'(z)$ . The bandwidth of the resonance in this filter was measured. Figure 16 shows the 3 dB bandwidth of the bandwidth-expanded

prediction error filter as a function of the resonance frequency. It can be seen that the bandwidth depends on the resonance frequency. The variation is some  $\pm 18\%$  about the mean bandwidth. Bandwidth expansion using LSF's gives inconsistent results.

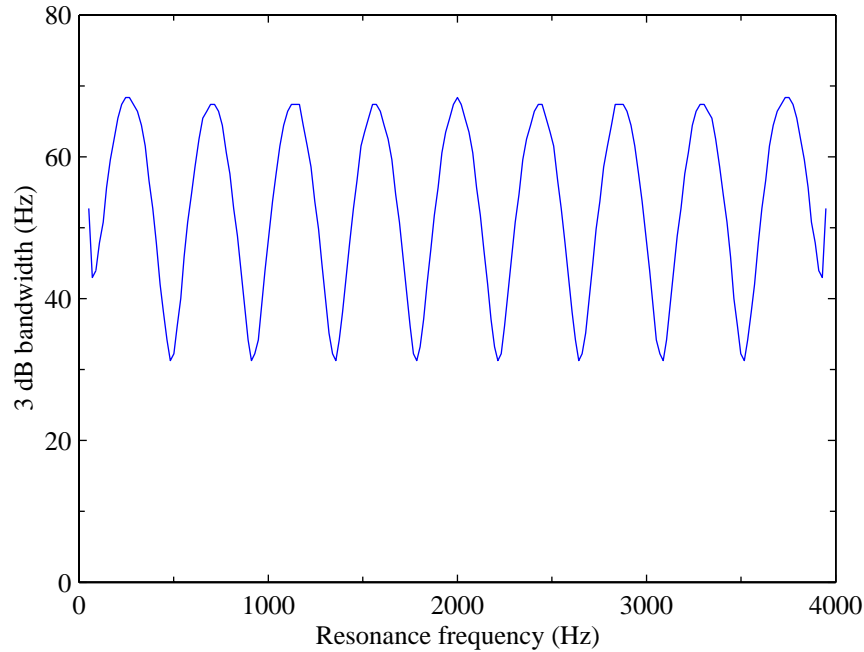


**Fig. 16** 3 dB bandwidth of the bandwidth-expanded prediction error filter as a function of the resonance frequency ( $r = 0.999$  and LSF modification factor  $\mu = 0.15$ ).

## 4 Summary

This report has demonstrated the problems of ill-conditioning of the LP equations for speech signals. The standard technique of white noise compensation brings the predictor coefficients to a reasonable range. This approach can be viewed as constraining the sum of the squared coefficients through a Lagrange multiplier. The other approaches to power spectrum modification (highpass noise, mixed highpass and white noise, and selective power spectrum modification) are all effective at controlling both the condition number of the correlation matrix and the range of predictor coefficients. However, white noise compensation still stands out as being both effective and simple to implement, while not imposing an excessive loss in prediction gain.

Methods which prematurely terminate the iterations for the solution of the correlation equations were also examined. In one approach, the prediction gain was limited to be below a threshold. In another approach, the absolute value of the reflection coefficients was limited to be below a

threshold. The Durbin recursion was halted at the point just before the threshold was exceeded and the prediction coefficients obtained at that point were used. For both strategies, the thresholds required to ensure that the resulting prediction coefficients were in a reasonable range ( $\pm 8$ ) resulted in significant performance loss for a substantial portion of the frames processed.

Bandwidth expansion to prevent abnormally narrow formant peaks can be provided by lag windowing of the correlation values. This approach has surprisingly little effect on the conditioning of the LP equations. Other approaches to bandwidth expansion are applied after LP analysis. We have compared the formulas to calculate the amount of bandwidth expansion due to a radial scaling of the singularities of the LP filter. A new simple formula for calculating the bandwidth expansion by spectral damping has been developed.

We have also examined a method to modify the spacing between line spectral frequencies for the purpose of bandwidth expansion. It is shown that this method is not consistent in the amount of bandwidth expansion across frequencies.

## Appendix A - Bandwidth of a Continuous-time Bandpass Filter

Consider the second-order bandpass filter

$$H(s) = \frac{s}{s^2 + (\Omega_o/Q)s + \Omega_o^2}. \quad (54)$$

This bandpass filter has zeros at  $s = 0$  and  $s = \infty$ . The poles occur at

$$s = -\frac{\Omega_o}{2Q}(1 \pm j\sqrt{4Q^2 - 1}). \quad (55)$$

The poles are complex for  $Q > 1/2$ . These complex conjugate poles are at a distance  $\Omega_o$  from the origin, with a real component equal to  $-\Omega_o/(2Q)$ . As  $Q$  increases beyond  $1/2$ , the poles move along a circle of radius  $\Omega_o$ .

The frequency response of the bandpass-filter can be written as

$$H(j\Omega) = \frac{Q/\Omega_o}{1 + jQ(\Omega/\Omega_o - \Omega_o/\Omega)}. \quad (56)$$

The maximum occurs for  $\Omega = \pm\Omega_o$ . The 3 dB points occur when  $|Q(\Omega/\Omega_o - \Omega_o/\Omega)| = 1$ . Let  $u = \Omega/\Omega_o$ . The 3 dB points satisfy

$$Q(u - \frac{1}{u}) = \pm 1 \quad \text{or} \quad Qu^2 \mp u - Q = 0. \quad (57)$$

This gives the solutions,

$$u = \frac{1}{2Q}(\pm 1 \pm \sqrt{1 + 4Q^2}). \quad (58)$$

The equation has four solutions, two positive and two negative. Consider the positive solutions,

$$u = \frac{1}{2Q}(\sqrt{1 + 4Q^2} \pm 1). \quad (59)$$

The two solutions are related by  $u_1 u_2 = 1$  and  $u_2 - u_1 = 1/Q$ . In terms of the 3 dB points  $\Omega_l$  and  $\Omega_u$ ,

$$\Omega_l \Omega_u = \Omega_o^2 \quad \text{and} \quad \Omega_u - \Omega_l = \Omega_o/Q. \quad (60)$$

The difference  $\Omega_u - \Omega_l$  is the 3 dB bandwidth of the resonance at frequency  $\Omega_o$ . Note that the response has a resonance even when the poles are real — the response is zero at zero frequency, rising to a maximum at  $\Omega_o$ , and falling to zero again for increasing frequency.

## Appendix B - Bandwidth of a Digital Bandpass Filter

The bilinear transformation relating a continuous-time filter to a discrete-time filter is

$$z = -\frac{s+a}{s-a} \quad \text{or} \quad s = a \frac{z-1}{z+1}. \quad (61)$$

Using the bilinear relationship, the 3 dB points in the response can be found for the digital filter. The frequency response point at  $s = j\Omega$  in the continuous-time system is mapped to the frequency point at  $z = e^{j\omega}$ , where

$$\omega = 2 \tan^{-1}(\Omega/a). \quad (62)$$

Consider the identity (valid for  $\theta_1\theta_2 > -1$ )

$$\tan^{-1}(\theta_1) - \tan^{-1}(\theta_2) = \tan^{-1}\left(\frac{\theta_1 - \theta_2}{1 + \theta_1\theta_2}\right). \quad (63)$$

The bandwidth for the resonance of the digital filter is then

$$\begin{aligned} \omega_u - \omega_l &= 2 \tan^{-1}(\Omega_u/a) - 2 \tan^{-1}(\Omega_l/a) \\ &= 2 \tan^{-1}\left(\frac{a(\Omega_u - \Omega_l)}{a^2 + \Omega_l\Omega_u}\right). \end{aligned} \quad (64)$$

This expression can be further simplified. The mapping of the poles is through the bilinear transformation. The poles at location  $s_1$  and  $s_2$  are mapped to poles at locations  $z_1$  and  $z_2$  with magnitudes  $r_1$  and  $r_2$ . The product of the magnitudes satisfy (from the bilinear transform)

$$r_1 r_2 = \frac{s_1 s_2 + a(s_1 + s_2) + a^2}{s_1 s_2 - a(s_1 + s_2) + a^2}. \quad (65)$$

The left side of this equation is  $z_1 z_2$  which is equal to  $r_1 r_2$  since the roots are either both real or complex conjugates of each other. Similarly the terms  $s_1 s_2$  and  $s_1 + s_2$  are real, since  $s_1$  and  $s_2$  are either both real or complex conjugates of each other. But from the formulation of the continuous-time filter,  $s_1 s_2 = \Omega_o^2$ , and  $s_1 + s_2 = -\Omega_o/Q$ . Furthermore in Appendix A, it was found that the 3 dB points of the continuous-time filter satisfy,

$$\Omega_l \Omega_u = \Omega_o^2 \quad \text{and} \quad \Omega_u - \Omega_l = \Omega_o/Q. \quad (66)$$

Then Eq. (65) becomes

$$r_1 r_2 = \frac{\Omega_l \Omega_u - a(\Omega_u - \Omega_l) + a^2}{\Omega_l \Omega_u + a(\Omega_u - \Omega_l) + a^2}. \quad (67)$$

This can be rearranged to become

$$\frac{1 - r_1 r_2}{1 + r_1 r_2} = \frac{a(\Omega_u - \Omega_l)}{a^2 + \Omega_l \Omega_u}. \quad (68)$$

Finally, using this in Eq. (64), the 3 dB bandwidth of the digital filter can be written as follows,

$$\begin{aligned} \omega_u - \omega_l &= 2 \tan^{-1} \left( \frac{1 - r_1 r_2}{1 + r_1 r_2} \right) \\ &= \pi/2 - 2 \tan^{-1}(r_1 r_2). \end{aligned} \quad (69)$$

## References

- [1] ITU-T Recommendation G.729 *Coding of Speech at 8 kbit/s Using Conjugate-Structure Algebraic-Code-Excited Linear-Prediction (CS-ACELP)*, March 1996.
- [2] 3GPP2 Document C.S0030-0, *Selectable Mode Vocoder Service Option of Wideband Spread Spectrum Communication Systems*, Version 2.0, Dec. 2001.
- [3] ITU-T Recommendation P.830 *Methods for Objective and Subjective Assessment of Quality*, Feb. 1996.
- [4] R. Salami, C. Laflamme, J.-P. Adoul, A. Kataoka, S. Hayashi, T. Moriya, C. Lamblin, D. Massaloux, S. Proust, P. Kroon, Y. Shoham, “Design and description of CS-ACELP: A toll quality 8 kb/s speech coder”, *IEEE Trans. Speech and Audio Processing*, vol. 6, pp. 116–130, March 1998.
- [5] R. D. Gitlin, J. F. Hayes, and S. B. Weinstein, *Data Communications Principles*. Plenum, 1992.
- [6] S. Haykin, *Adaptive Filter Theory*, 4<sup>th</sup> ed., Prentice-Hall, 2002.
- [7] G. H. Golub and C. F. Van Loan, *Matrix Computations*, 3<sup>rd</sup> ed., John Hopkins University Press, 1996.
- [8] R. M. Gray, “Toeplitz and Circulant Matrices: A Review”, Web document available from <http://www-isl.stanford.edu/~gray/>, March 2000.
- [9] B. S. Atal and M. R. Schroeder, “Predictive coding of speech signals and subjective error criteria,” *IEEE Trans. Acoustics, Speech, Signal Processing*, vol. ASSP-27, pp. 247–254, June 1979.
- [10] Y. Tohkura, F. Itakura, and S. Hashimoto, “Spectral smoothing technique in PARCOR speech analysis-synthesis,” *IEEE Trans. Acoustics, Speech, Signal Processing*, vol. ASSP-26, pp. 587–596, Dec. 1978.
- [11] Y. Tohkura and F. Itakura, “Spectral sensitivity analysis of PARCOR parameters for speech data compression,” *IEEE Trans. Acoustics, Speech, Signal Processing*, vol. ASSP-27, pp. 273–280, June 1979.
- [12] R. Viswanathan and J. Makhoul, “Quantization properties of transmission parameters in linear predictive systems,” *IEEE Trans. Acoustics, Speech, Signal Processing*, vol. ASSP-23, pp. 309–321, June 1975.
- [13] K. K. Paliwal and W. B. Kleijn, “Quantization of LPC parameters,” in *Speech Coding and Synthesis* (W. B. Kleijn and K. K. Paliwal, eds.), ch. 12, pp. 433–466, Elsevier, 1995.
- [14] H. Tasaki, K. Shiraki, K. Tomita, and S. Takahashi, “Spectral postfilter design based on LSP transformation,” *Proc. IEEE Workshop on Speech Coding* (Pocono Manor, PA), pp. 57–58, Sept. 1997.